Technique for Improving Detection of WSR-88D Mesocyclone Signatures by Increasing Angular Sampling

VINCENT T. WOOD AND RODGER A. BROWN

NOAA/National Severe Storms Laboratory, Norman, Oklahoma

DALE SIRMANS

System Technology Associates, Inc., Norman, Oklahoma

14 October 1999 and 10 July 2000

ABSTRACT

The Doppler velocity signature of a thunderstorm mesocyclone becomes increasingly degraded as distance from the radar increases. Degradation is due to the broadening of the radar beam with range relative to the size of the mesocyclone. Using a model mesocyclone and a simulated WSR-88D Doppler radar, a potential approach for improving the detection of mesocyclones is investigated. The approach involves decreasing the azimuthal sampling interval from the conventional 1.0° to 0.5°. Using model mesocyclones that cover the spread of expected mesocyclone sizes and strengths, simulations show that stronger mesocyclone signatures consistently are produced when radar data are collected at 0.5° azimuthal increments. Consequently, the distance from the radar at which a mesocyclone of a given strength and size can be detected increases by an average of at least 50% when data are collected using 0.5° azimuthal increments.

The simulated findings are tested using Archive Level I (time series) data collected by the WSR-88D Operational Support Facility's KCRI radar during the Oklahoma–Kansas tornado outbreak of 3 May 1999. With the availability of time series data, an Archive Level II dataset was produced for both 1.0° and 0.5° azimuthal intervals. One-third of the mesocyclone signatures collected using 0.5° azimuthal intervals were 10% to over 50% stronger than their 1.0° azimuthal interval counterparts.

1. Introduction

An inherent characteristic of any Doppler weather radar, including the Weather Surveillance Radar-1988 Doppler (WSR-88D), is that detection resolution of thunderstorm mesocyclones degrades with range. The problem arises owing to the widening of the radar beam with range relative to vortex size (Donaldson 1970; Brown and Lemon 1976; Burgess et al. 1993).

Burgess (1976) and Burgess and Donaldson (1979) present data that suggest that 0.5° azimuthal sampling improves mesocyclone detection at far ranges. However, it is not clear how much the detection capability would be improved using 0.5° azimuthal sampling compared to the conventional 1.0° azimuthal sampling of the WSR-88D.

The purpose of this paper is to quantify improvement that could be realized in WSR-88D detection of mesocyclones by decreasing the azimuthal sampling interval from 1.0° to 0.5°. In this study, simulated Doppler velocity measurements were produced by scanning a simulated Doppler radar through an analytical velocity field characterized by the Rankine (1901) combined vortex. Nine simulated mesocyclones are used to represent the full range of likely mesocyclone sizes and strengths. The sizes and strengths of the resulting mesocyclone signatures are then compared for 1.0° and 0.5° azimuthal sampling intervals. Finally, the simulated findings are confirmed using data collected by a WSR-88D using both 1.0° and 0.5° azimuthal intervals.

2. Doppler radar simulation

For the WSR-88D system, an azimuthal sampling interval of 0.5° can be achieved in several ways. First, one could halve the number of transmitted pulses per sampling volume while keeping the same antenna rotation rate used for 1.0° azimuthal sampling. Second, one could decrease the antenna rotation rate while retaining the same number of pulses per sampling volume used for 1.0° azimuthal sampling. Third, one could use some combination of these two options.

The most practical way for an operational WSR-88Ds to collect 0.5° azimuthal data is to decrease the number

Corresponding author address: Vincent T. Wood, National Severe Storms Laboratory, 1313 Halley Circle, Norman, OK 73069.
E-mail: wood@nssl.noaa.gov

TABLE 1. Relative effect of azimuthal sampling interval (ΔAZ) on radar performance based on the mean effective beamwidth of WSR-88Ds; the mean antenna pattern beamwidth is 0.89°. It is assumed that there is a proportional decrease in the number of transmitted pulses as ΔAZ decreases.

ΔAZ	Effective one-way beamwidth BW_e	Ratio of resolution scale ($=BW_e/1.39°$)	Range ratio ($=1.39°/BW_e$)	Ratio of estimate standard deviation $[=(1°/\Delta AZ)^{1/2}]$
1.0°	1.39°	1	1	1
0.75°	1.18°	0.85	1.18	1.15
0.5°	1.03°	0.74	1.35	1.41
0.25°	0.93°	0.67	1.49	2

of pulses by one-half while maintaining the same antenna rotation rate used for 1.0° azimuthal sampling. This is achievable as long as there are enough pulses to compute reliable reflectivity, Doppler velocity, and spectrum width estimates. In practice, it might be feasible to use slightly slower antenna rotation rates with 0.5° azimuthal intervals for elevation angles below about 7° (upper limit of long-range detection) and use 1.0° azimuthal intervals at a faster rotation rate for the higher elevation angles. Though tailored specifically for WSR-88D operational parameters, the results shown in this paper are generally applicable to any Doppler radar.

a. Assumptions

The analytical simulation of a WSR-88D, developed by Wood and Brown (1997), and the Rankine combined vortex model of a mesocyclone were used to produce simulated Doppler velocity measurements. Assumptions made in the simulation are 1) the tangential velocity distribution across the mesocyclone is approximated by an axisymmetric Rankine combined velocity profile, 2) the tangential velocity field is uniform with height, 3) reflectivity is uniform across the mesocyclone, and 4) the radar beam pattern is Gaussian shaped.

b. Modification

One modification was made to the radar simulation described by Wood and Brown (1997). For range-gate depth, the weighting function for the transmitter power pulse, $W(r)$, is approximated by a trapezoidal shape. The top of the trapezoid, where the weight is 1.0, has a range depth of 180 m. The base of the trapezoid, where the weight is 0.0, has a range depth of 260 m.

c. Effective beamwidth

The mean antenna pattern beamwidth of the operational WSR-88Ds is 0.89°. However, since the radar antenna is moving while transmitting and receiving the number of pulses required to calculate a representative Doppler velocity value, beamwidth is effectively broadened in the azimuthal direction. The broadened beamwidth is called the *effective* beamwidth (e.g., Doviak and Zrnic 1993). By convention, beamwidth is defined as the width of the *one-way* beam where the transmitted power is one-half of the peak value. However, when one wants to study the effects of the beamwidth on the resolution of radar measurements, it is more appropriate to use the *two-way* half-power beamwidth determined by the two-way antenna pattern. A procedure for computing the effective beamwidth consists of taking the antenna two-way pattern [as the square of the Gaussian approximation of the one-way pattern (Probert-Jones 1962)] and convolving it with the uniform sampling interval in azimuth (ΔAZ). Results of this convolution for the mean beamwidth of the operational WSR-88Ds are given in Table 1; information also has bean added for ΔAZ of 0.75° and 0.25° to give a better picture of overall trends. As seen, the effective one-way beamwidth is 1.39° for 1.0° azimuthal sampling and 1.03° for 0.5° azimuthal sampling. Since data acquisition over a finite azimuthal sampling interval results in an effective beamwidth greater than the antenna pattern beamwidth, the resulting two-dimensional effective antenna pattern is elliptical with the major (minor) axis lying in the azimuth (elevation) direction.

The relative effect of azimuth sampling interval on radar performance is tabulated in Table 1. There is a significant improvement in resolution (i.e., smaller scales are detectable) with decrease of ΔAZ from 1.0° to 0.5°. However, there is relatively little further improvement with ΔAZ values less than 0.5°, since ΔAZ is small compared to antenna pattern width. Subjectively, it appears the best ''trade-off'' between resolution and estimate standard deviation is ΔAZ of 0.5°.

d. Random noise

As the number of transmitted and received pulses decreases, the noisiness (variance) of the Doppler velocity estimate increases. To approximate the effect of halving the number of pulses to produce 0.5° sampling, the standard deviation of the Gaussian-distributed white noise (mean of zero) being added to each computed Doppler velocity value was increased by $(1.0°/0.5°)^{1/2}$ or 1.41 (see Table 1). Based on typical WSR-88D operating characteristics, the standard deviation of the Doppler velocity estimate is approximately 0.7 m s^{-1} for 1.0° azimuthal sampling (determined from Fig. 6.5 of Doviak and Zrnic 1993). The typical standard deviation then increases to 1.0 m s^{-1} for 0.5° azimuthal

sampling. Both of these standard deviations are within the specification of no more than 1.0 m s^{-1} at input spectrum width of 4.0 m s^{-1} (e.g., Heiss et al. 1990).

3. Comparisons for an average-sized mesocyclone

a. Basic features

Initially, simulations of Doppler radar data are presented to compare 0.5° and 1.0° azimuthal sampling for the detection of an average-sized mesocyclone; a wider range of sizes and strengths are considered in section 4. The model mesocyclone has a peak rotational velocity (V_x) of 25 m s^{-1} at a core diameter (D) of 5 km. From the Doppler velocity simulations, it is possible to deduce a mean rotational velocity and core diameter for the resulting mesocyclone signature. The deduced mean rotational velocity ($\overline{V}_{rot}$) is one-half the difference between the extreme positive and negative Doppler velocity values in the mesocyclone signature. The deduced core diameter (CD) is the distance between the same extreme Doppler velocity values.

Figure 1 shows simulated data collection for 1.0° and 0.5° azimuthal increments. The data points represent one possible placement (of many) of the data points relative to the peaks of the smooth curve. There are two advantages of 0.5° azimuthal data collection over 1.0° data collection portrayed in Fig. 1; for the sake of illustration, noise was not added to the data points. First, the smooth-peaked curves (with data points along them) represent the Doppler-velocity azimuthal profile of the mesocyclone signature if the radar were able to make measurements in a continuous manner across the mesocyclone. Owing to the fact that the effective beamwidth is smaller for 0.5° azimuthal data collection (1.03° vs 1.39°; see Table 1), the 0.5° curve is less degraded relative to model peak velocity of 25 m s^{-1} (pointed curve). This means that a stronger mesocyclone signature is produced with 0.5° azimuthal sampling.

The second advantage of 0.5° azimuthal data collection is that there are twice as many data points available with which to define the peaks of the mesocyclone signature curve. Having twice as many data points improves the azimuthal resolution. In Fig. 1a, the extreme data points of −15.4 and +17.0 m s^{-1} produce a deduced mean rotational velocity ($\overline{V}_{rot}$) of 16.2 m s^{-1} and a CD of 7.9 km. In Fig. 1b, the greater datapoint density (in conjunction with the less degraded signature curve) produces extreme data points of −19.3 and 18.6 m s^{-1}. The resulting deduced mean rotational velocity of 19.0 m s^{-1} and deduced core diameter of 5.2 km are much closer to the true model values.

b. Variations with range

For the remainder of the simulations in this paper, random noise (discussed above) was added to the simulated data points before deduced mean rotational velocities and core diameters were computed. Figure 2 shows the variations of deduced velocities and diameters as a function of range for azimuth increments (ΔAZ) of 1.0° and 0.5°. The overall trend of velocities is to decrease with increasing range, while the trend for diameters is to increase with range.

The vertical width of the shaded bands in Figs. 2a and 2b represents the full spread of mean rotational velocity measurements that are likely to occur for the various possible placements of the radar beam with respect to the mesocyclone's peak rotational velocities. The spread is produced by computing $\overline{V}_{rot}$ values for all

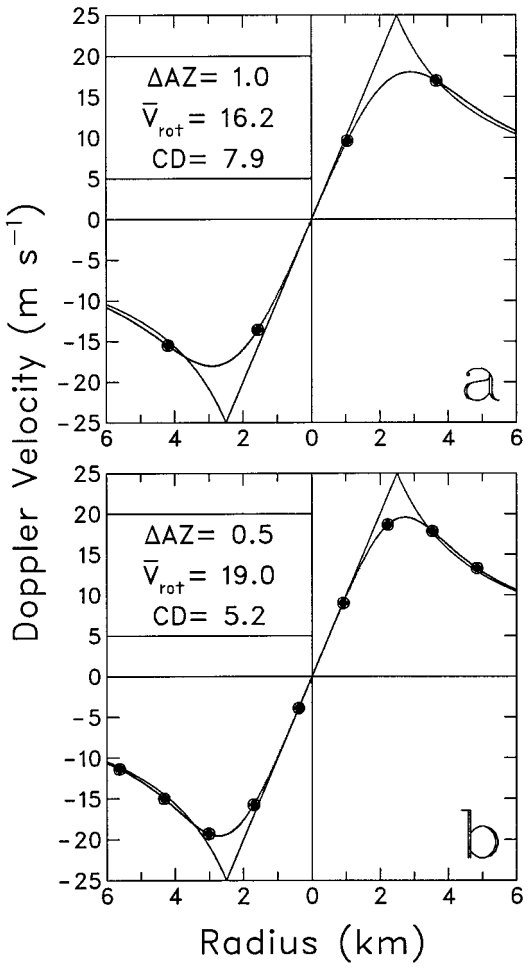

FIG. 1. Relationships of data points relative to the azimuthal profiles of a Doppler-velocity mesocyclone signature for azimuthal sampling intervals (ΔAZ) of (a) = 1.0° and (b) = 0.5°. The curve with rounded peaks (along which the data points fall) represents the Doppler-velocity azimuthal profile of the mesocyclone signature if the radar were able to make measurements in a continuous manner across the mesocyclone at a range of 150 km. Data points (black dots) represent the locations of successive Doppler velocity measurements collected at ΔAZ increments as the radar beam scans across the mesocyclone. The model azimuthal profile is indicated by the curve with pointed peaks corresponding to the typical mesocyclone having a peak tangential velocity of 25 m s^{-1} at a core diameter of 5 km. Deduced values of mean rotational velocity ($\overline{V}_{rot}$) in m s^{-1} and core diameter (CD) in km are indicated.

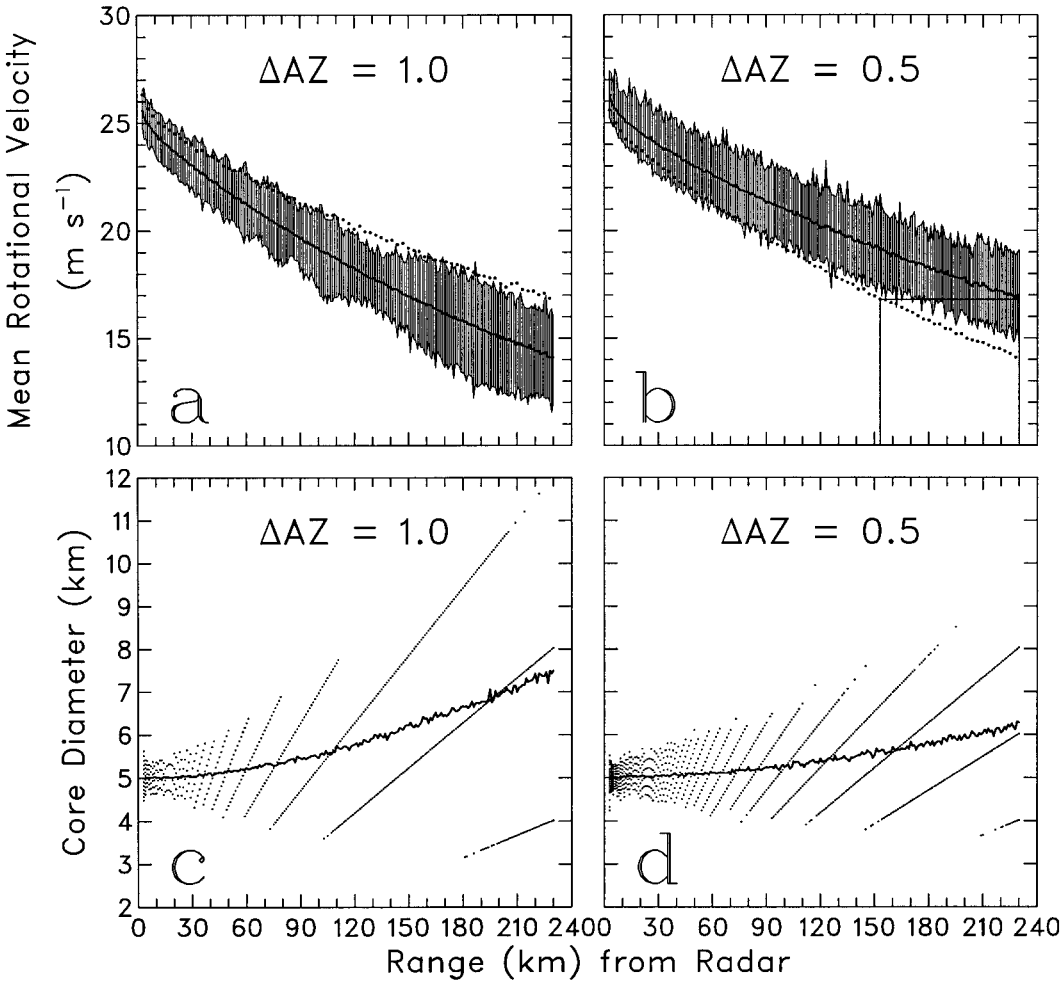

FIG. 2. Variations of (a) and (b) deduced mean rotational velocity and (c) and (d) deduced core diameter values for the typical mesocyclone signature as a function of range for 1.0° and 0.5° azimuthal sampling (ΔAZ). Gaussian white noise was added to the individual Doppler velocity data points used to compute the mean rotational velocity and core diameter. In (a) and (b), the shaded band's vertical width represents the full spread of possible velocity values arising from the chance placement of the radar beam relative to the peaks of the signature curve; values were computed for 51 positions equally spaced over the ΔAZ interval. The jagged solid curve in the middle of the velocity band represents the average of the $\overline{V}_{rot}$. In (a), the dotted curve corresponds to the solid curve in (b); the dotted curve in (b) corresponds to the solid curve in (a). In (c) and (d), the lines of data points represent the number of possible core diameters at each range. The jagged curve through the middle of the lines represents the average of the deduced core diameter values.

possible azimuthal sampling offsets between the data points and mesocyclone center with the inclusion of Gaussian-distributed random noise (e.g., Wood and Brown 1997). Even though the 0.5° simulation contains more added noise, the widths of the two bands are comparable. The increased noisiness is compensated by the reduced variations owing to the more closely spaced 0.5° interval data points. The solid curve in the middle of the data band is the average of all possible mean rotational velocity values at each range. The dotted curve represents the solid curve from the other ΔAZ band. The shaded bands reveal that the magnitudes of rotational velocity estimates are larger and closer to their model values of 25 m s^{-1} when data are collected using 0.5° versus 1.0° azimuthal sampling.

While the deduced mean rotational velocity for the average-sized mesocyclone can take on many possible values at a given range depending on the placement of the data points relative to the peaks of the mesocyclone signature (Figs. 2a and 2b), the deduced core diameter has only a finite number of possible values that decrease in number with increasing range (Figs. 2c and 2d). Both the spread of possible diameters and the mean value (jagged line through middle of values) increase with range because the distance between ΔAZ data points increase with range. The reasons for the behavior of the deduced core diameters are more complicated and are discussed in detail by Wood and Brown (2000).

The locations of the average curves (solid and dotted) relative to the shaded bands in Figs. 2a and 2b suggest that there is considerable overlap of mean rotational velocity values between 1.0° and 0.5° azimuthal data

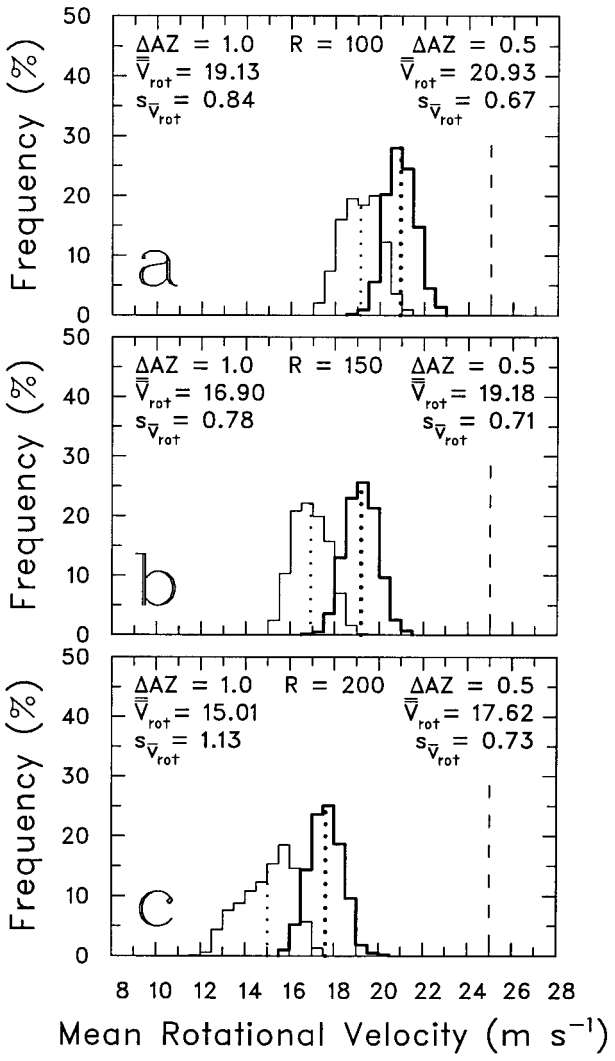

FIG. 3. Frequency distributions of mesocyclone mean rotational velocity estimates across the bands in Fig. 2 at (a) 100-, (b) 150-, 2nd (c) 200-km range. The thin (thick) lines correspond to the 1.0° (0.5°) azimuthal data collection. The average of the $\overline{V}_{rot}$ values ($\overline{\overline{V}}_{rot}$) is indicated by the vertical dotted line. The vertical dashed line represents the peak tangential velocity of the model mesocyclone. The standard deviation of mean rotational velocity is given by $s_{\overline{V}_{rot}}$ (m s^{-1}).

collection. However, the velocity distributions across the bands are more Gaussian shaped than uniform. The frequency distributions of deduced mean rotational velocities for 1.0° and 0.5° azimuthal data collection are presented at three ranges in Fig. 3.

The distributions in Fig. 3 reveal that there is less variation (i.e., a smaller standard deviation) among the various estimates of the mean rotational velocity with 0.5° azimuthal sampling. With increasing range, the overall average values of the two mean rotational velocity distributions become farther apart, for example, the difference increasing from 1.80 m s^{-1} at 100 km to 2.28 m s^{-1} at 150 km to 2.61 m s^{-1} at 200 km. Only a small fraction of the possible mean rotational velocity values within the two distributions actually overlap. The percentages of 0.5° mean rotational velocities that are larger than all of the 1.0° velocities are 77%, 87%, and 86% at 100, 150, and 200 km, respectively. This means that, at least for the average-sized mesocyclone, using an azimuthal sampling interval of 0.5° produces distinctly stronger mesocyclone signatures.

TABLE 2. Nine selected model mesocyclones having a variety of peak rotational velocities and core diameters.

Model mesocyclone	Core diameter (km)	Peak rotational velocity (m s^{-1})
A	2.5	12.5
B	2.5	25
C	2.5	50
D	5	12.5
E	5	25
F	5	50
G	10	12.5
H	10	25
I	10	50

4. Comparisons for mesocyclones having varying sizes and strengths

Having shown significantly improved detection capability for an average-sized mesocyclone using an azimuthal increment of 0.5°, an investigation was undertaken of mesocyclones having a wider range of sizes and strengths. The characteristics of nine selected model mesocyclones having three different peak rotational velocities and three different core diameters are listed in Table 2. Mesocyclone E is the same mesocyclone discussed in section 3.

It is possible to quantify theoretically how much mesocyclone detection improves with 0.5° azimuthal sampling by selecting common threshold velocities for average $\overline{V}_{rot}$ values (the line through the center of the band) and determining how much farther in range values equal to the threshold value can be detected. For example, the horizontal line in the bottom-right portion of Fig. 2b represents a threshold value of 17 m s^{-1} that connects the centerlines of the two bands. With a ΔAZ of 1.0°, the centerline value of 17 m s^{-1} is at a range of 153 km, while the centerline value with a ΔAZ of 0.5° is at 230 km. This means that for a mesocyclone having true core rotation of 25 m s^{-1} and a detection threshold of 17 m s^{-1}, the increased horizontal resolution provided by 0.5° sampling extends the average range of mesocyclone detection by 50%.

The ratios of range for 0.5° azimuthal sampling ($R_{0.5}$) to the range for 1.0° azimuthal sampling ($R_{1.0}$) for various threshold values of average $\overline{V}_{rot}$ for the nine model mesocyclones are shown in Fig. 4. For each peak rotational velocity (V_x), the ratios associated with the three

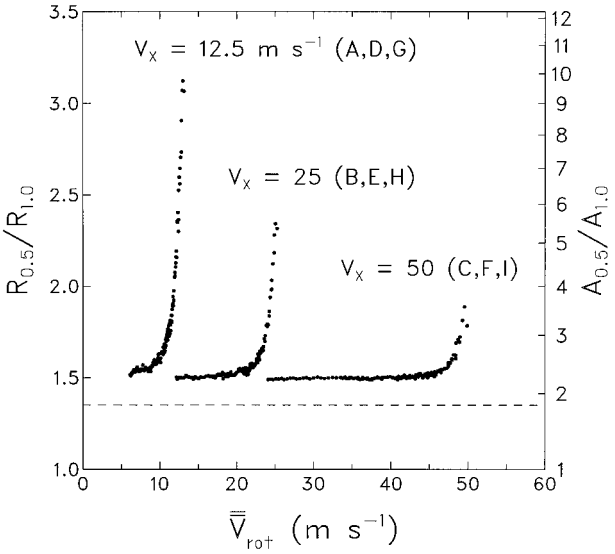

FIG. 4. Ratios of range $R_{0.5}$ for 0.5° azimuthal data collection to range $R_{1.0}$ for 1.0° azimuthal data collection as a function of the average of mean rotational velocities (indicated by $\overline{\overline{V}}_{rot}$) for the nine model mesocyclones. Corresponding ratios of coverage area ($A_{0.5}/A_{1.0}$) are indicated along the right side of the figure. The data points have been smoothed using a seven-point running mean. For a given model peak rotational velocity (V_x), the ratios associated with the three model core diameters (D) successively overlapped to produce one continuous curve.

model core diameters successively overlapped to produce one continuous curve. The range increase is at least 50% (ratio of 1.5) for all threshold values with 0.5° azimuthal sampling. As the threshold value approaches the peak velocity value (i.e., as range from the radar approaches zero), the ratio increases. This increase is due to range in the denominator (1.0°) approaching zero faster than range in the numerator (0.5°), because 1.0° values are smaller than 0.5° values, as indicated in Figs. 2a and 2b. The dashed horizontal line indicates the theoretical range improvement of 1.35 based on the ratio of the effective beamwidths for 1.0° and 0.5° azimuthal sampling (see Table 1). An additional improvement owing to the finer azimuthal resolution with 0.5° azimuthal sampling results in an increased range ratio of at least 1.5. Regardless of mesocyclone size or strength, the detection range for any velocity threshold value is at least 50% farther from the radar using 0.5° azimuthal sampling.

The results of these simulations have important implications for mesocyclone detection at long range. In terms of horizontal coverage, the area exceeding a particular threshold value is essentially doubled using 0.5° azimuthal sampling, which is very significant from an operational perspective. This is reflected in the ratio of coverage area at 0.5° azimuthal increment ($A_{0.5}$) to coverage area at 1.0° azimuthal increment ($A_{1.0}$), as shown in Fig. 4. However, to keep these results in perspective, it is important to remember that beyond a range of about 160 km the WSR-88D's lowest elevation angle (0.5°) is greater than 3 km above the ground. At these ranges, only the midaltitude portion of the mesocyclone is detectable. Even though low-altitude mesocyclone data are not available, the mesocyclone signature at midaltitudes will be stronger for 0.5° azimuthal sampling.

5. Comparisons using actual WSR-88D data

During the Oklahoma–Kansas tornado outbreak of 3 May 1999, Archive Level I (time series) data were collected at the WSR-88D Operational Support Facility's (OSF) KCRI radar site in Norman. The National Center for Atmospheric Research recently developed software for the OSF that permits recording the basic pulse-by-pulse time series data from a WSR-88D. The Archive Level I recorder was attached to the KCRI radar and made available for this study. After running a few short tests to become familiar with the time series recording equipment, the first full-fledged data recording took place on 3 May 1999. Being interested in mesocyclone and tornadic vortex signatures at lower altitudes for this ''test case,'' data were recorded at elevation angles between 0.5° and 2.0° for 6 h. Data from some mesocyclones on 3 May 1999 were not collected due to Archive Level I recorder malfunctions and to a half-hour power failure.

With time series data, it is possible to produce two Archive Level II datasets of radar parameters for the same storm situation—one having 0.5° azimuthal sampling and the other having 1.0° azimuthal sampling. For a given antenna rotation rate and pulse repetition frequency, the azimuthal sampling interval is controlled by the number of pulses used to compute a mean Doppler velocity value. Thus, 0.5° azimuthal data collection was achieved by processing half the number of pulses required for 1.0° azimuthal data collection. The 0.5° and 1.0° data computed in this manner were used to verify the simulated findings reported in this study.

Figure 5 compares the improvement of 0.5° sampling over 1.0° sampling by computing the ratios of mean rotational velocity $\overline{V}_{0.5}$ at 0.5° azimuthal data collection to mean rotational velocity $\overline{V}_{1.0}$ at 1.0° azimuthal data collection. Solid curves based on the nine model mesocyclones are plotted in the figure. The curves are the ratios of the averages of the types of velocity distributions shown in Fig. 3; in particular, curve E is the ratio of the average lines through the centers of the shaded bands in Figs. 2a and 2b. The ratios increase with range more rapidly for smaller mesocyclones than for larger ones, regardless of mesocyclone strength. The long–short dashed curves represent the extreme ratios that would be expected. Based on frequency distributions like those shown in Fig. 3, the lower long–short dashed curve represents the ratio of the smallest rotational velocity for the 0.5° distribution to the largest rotational velocity for the 1.0° distribution for mesocyclone I. Likewise, the upper long–short dashed curve represents the ratio of the largest rotational velocity for

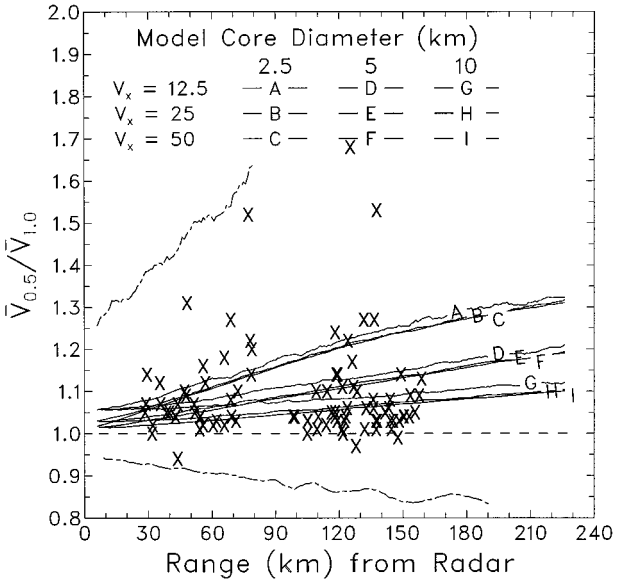

FIG. 5. Ratios of mean rotational velocity $\bar{V}_{0.5}$ at 0.5° azimuthal data collection to mean rotational velocity $\bar{V}_{1.0}$ at 1.0° azimuthal data collection. The lettered curves represent the ratios of the averages of the mean rotational velocities for the nine model mesocyclones as a function of range. The long–short dashes represent extreme ratios based on the simulations. The simulated data have been smoothed using a nine-point running mean. Horizontal dashed line indicates no improvement using 0.5° azimuthal sampling. Superimposed ×s are the actual ratios for 91 mesocyclone velocity signatures measured on 3 May 1999 for 0.5° and 1.0° azimuthal sampling.

the 0.5° distribution to the smallest rotational velocity for the 1.0° distribution for mesocyclone A.

The ×s plotted in Fig. 5 are the actual ratios for 91 mesocyclone signatures recorded on 3 May 1999 using the KCRI radar. All of the actual ratios fall within the theoretical limits indicated by the long–short dashed curves. Based on the chance placement of the 0.5° and 1.0° azimuthal data points relative to the peaks of the mesocyclone signature, one would expect most of the observed ratios to be above the dashed 1.0 ratio line, with a few of them falling below the line. This is the situation portrayed in Fig. 5.

About two-thirds of the observed ratios fall between values of 1.0 and 1.1. This means that, in most situations, the mean rotational velocity is up to 10% stronger using 0.5° azimuthal intervals. Most of the remaining one-third of the ratios have values between 1.1 and 1.68. Thus, one-third of the 0.5° mesocyclone signatures have mean rotational velocities that are 10%–68% stronger than their 1.0° azimuthal interval counterparts. These results clearly confirm the simulated findings that stronger mesocyclone signatures arise when WSR-88D data are collected using 0.5° azimuthal sampling.

6. Concluding discussion

Both realistic simulations and prototype WSR-88D measurements were undertaken to determine whether detection of mesocyclones can be improved by collecting data at 0.5° rather than the conventional 1.0° azimuthal intervals. The finer azimuthal resolution can be achieved by halving the number of transmitted pulses while, at the same time, keeping the standard error of the Doppler velocity estimates within the specified limits. Following are the key findings of the study.

- A stronger mesocyclone signature is produced using 0.5° azimuthal sampling because (a) the effective beamwidth resulting from 0.5° azimuthal sampling is narrower than that for 1.0° azimuthal sampling, and (b) with twice the azimuthal density of data points, there is better sampling of the peaks of the mesocyclone signature.
- Regardless of mesocyclone strength and size, the mesocyclone signature theoretically can be detected at least 50% farther away from the radar with 0.5° azimuthal sampling. In terms of horizontal coverage, the area exceeding a particular threshold value is essentially doubled using 0.5° azimuthal sampling, which is very significant from an operational perspective.
- Actual data collected with the WSR-88D KCRI radar during the Oklahoma–Kansas tornado outbreak of 3 May 1999 confirm the simulated theoretical findings of improved mesocyclone detection with 0.5° azimuthal sampling. One-third of the mesocyclone velocity signatures are 10% to over 50% stronger than their 1.0° azimuthal interval counterparts.

Acknowledgments. The authors appreciate the efforts of Harold Brooks, Don Burgess, and Jeff Trapp of the NSSL for reviewing and providing helpful comments and suggestions on an earlier version of this manuscript. The authors acknowledge the anonymous reviewers for contributing valued comments and suggestions that led to the improvement of the manuscript. The authors thank Joe VanAndel of National Center for Atmospheric Research for developing software to record the basic pulse-by-pulse time series (Archive Level I) data and Rick Rhoton of System Technology Associates, Inc., for processing data collected by KCRI radar in Norman. This study was partially funded by the WSR-88D Operational Support Facility in Norman, Oklahoma.

REFERENCES

Brown, R. A., and L. R. Lemon, 1976: Single Doppler radar vortex recognition. Part II: Tornadic vortex signatures. Preprints, *17th Conf. on Radar Meteorology,* Seattle, WA, Amer. Meteor. Soc., 104–109.

Burgess, D. W., 1976: Single Doppler radar vortex recognition. Part I: Mesocyclone signatures. Preprints, *17th Conf. on Radar Meteorology,* Seattle, WA, Amer. Meteor. Soc., 97–103.

——, and R. J. Donaldson Jr., 1979: Contrasting tornadic storm types. Preprints, *11th Conf. on Severe Local Storms,* Kansas City, MO, Amer. Meteor. Soc., 189–192.

——, ——, and P. R. Desrochers, 1993: Tornado detection and warning by radar. *The Tornado: Its Structure, Dynamics, Prediction, and Hazards, Geophys. Monogr.,* No. 79, Amer. Geophys. Union, 203–221.

Donaldson, R. J., Jr., 1970: Vortex signature recognition by a Doppler radar. *J. Appl. Meteor.,* **9,** 661–670.

Doviak, R. J., and D. S. Zrnic, 1993: *Doppler Radar and Weather Observations.* Academic Press, 562 pp.

Heiss, W. H., D. L. McGrew, and D. Sirmans, 1990: NEXRAD: Next Generation Weather Radar (WSR-88D). *Microwave J.,* **33,** 79–80, 84–98.

Probert-Jones, J. R., 1962: The radar equation in meteorology. *Quart. J. Roy. Meteor. Soc.,* **88,** 485–495.

Rankine, W. J. M., 1901: *A Manual of Applied Mechanics.* 16th ed. Charles Griff and Company, 680 pp.

Wood, V. T., and R. A. Brown, 1997: Effects of radar sampling on single-Doppler velocity signatures of mesocyclones and tornadoes. *Wea. Forecasting,* **12,** 928–938.

——, and ——, 2000: Oscillations in mesocyclone signatures with range owing to azimuthal radar sampling. *J. Atmos. Oceanic Technol.,* **17,** 90–95.